Hindawi
Advances in Mathematical Physics
Volume 2022, Article ID 2656836, 15 pages
https://doi.org/10.1155/2022/2656836

Research Article

Function Projective Synchronization of Two Complex Networks with Unknown Sector Nonlinear Input and Multiple Time-Varying Delay Couplings

Na Fang,[1] Da Wei,[2] Nan-nan Yin,[2] Dan-ying Xu,[3] Hua Liu,[4] and Jie Fang[2]

[1]*College of Software Engineering, Zhengzhou University of Light Industry, Zhengzhou 450002, China*
[2]*College of Electrical and Information Engineering, Zhengzhou University of Light Industry, Zhengzhou 450002, China*
[3]*State Grid Henan Electric Power Company, Xuchang Power Supply Company, Xuchang 461000, China*
[4]*State Grid Henan Electric Power Company, Zhengzhou 450052, China*

Correspondence should be addressed to Jie Fang; fang0511jie@126.com

Received 26 March 2022; Accepted 16 July 2022; Published 8 August 2022

Academic Editor: Ghulam Rasool

This paper deals with the function projective synchronization of two complex dynamic networks with unknown sector nonlinear input, multiple time-varying delay couplings, model uncertainty, and external interferences. Based on Lyapunov stability theory and inequality transformation method, the robust adaptive synchronization controller is designed, by which the drive and response systems can achieve synchronization according to the function scaling factor. Different from some existing studies on nonlinear system with sector nonlinear input, this paper studies the synchronization of two complex dynamic networks when the boundary of sector nonlinear input is unknown. The controller does not include the boundary value of the sector nonlinear input and the time delay term, so it is more practical and relatively easy to implement. The corresponding simulation examples demonstrate the effectiveness of the proposed scheme.

1. Introduction

There are all kinds of complex systems in nature world. These complex systems can be seen as networks, such as Internet, power grid, communication networks, transportation networks, ecological networks, and social networks. The dynamic behavior of complex networks affects almost every aspect of our lives. Among many researches on complex networks, synchronization research is one of the most important branches. So far, many types of synchronization have been investigated, such as complete synchronization [1, 2], antisynchronization [3], exponential synchronization [4–6], quasisynchronization [7], lag synchronization [8, 9], combined synchronization [10], projection synchronization [11], and function projection synchronization [12–14]. Function projection synchronization is a general synchronization form, which means that the driving system and the response system can be synchronized according to a certain function proportional relationship. The complete synchronization, antisynchronization, and projection synchronization are all its exceptional cases. Function projection synchronization has attracted widespread attention because of its implied application in information science and secure communication [15, 16].

It is well known that various time delays are unavoidable in actual engineering applications. The time delay may destroy the dynamic characteristics and decrease the stability of the system, which is extremely detrimental to the control system [17–19]. Multiple time-varying delay couplings mean that multiple different time-varying delays exist in the complex network. The description of multiple time-varying delay couplings is a general description of time delay, and the constant time-delay couplings and single time-varying delay couplings are its special circumstances. The synchronization researches of complex networks with multiple time-varying delay couplings are more realistic and representative [20, 21]. Zhang et al. [22] researched the synchronization of uncertain complex networks with time-varying node delay and multiple time-varying coupling delays via the adaptive control. In [23], the authors researched the synchronization in nonlinear complex networks with multiple time-varying delays. Wang et al. [24] studied the lag synchronization between two coupled complex networks with multiple time-varying delays via the adaptive pinning control. Zhao et al. [25] studied the synchronization issue of uncertain complex networks with multiple time-varying delays. Lu et al. [26] established a robust adaptive synchronization scheme for general complex networks with multiple time-varying coupling delays and uncertainties. Guan et al. [27] studied the synchronization of complex networks with system delay and multiple time-varying coupling delays via impulsive distributed control.

In the actual control system, the backlash, friction, dead zone, and hysteresis will cause the nonlinearity of the control input, which lead to system instability or control performance degeneration [28–34]. Therefore, the synchronization researches of complex networks with input nonlinearity are meaningful. Sector nonlinear input is one type of the nonlinear input, which means that the system input is in a fan-shaped area. Sector nonlinear input represents a large type of input nonlinearity. Many scholars have studied the control of nonlinear systems with sector nonlinear input. Boulkroune and Msaad [35] researched the adaptive variable-structure control of uncertain chaotic MIMO systems with both sector nonlinearities and dead-zones. Fang et al. [36] researched the modified projective synchronization of chaotic systems with sector nonlinearities input. Boubellouta et al. [37] achieved synchronization for a class of fractional-order chaotic systems with sector nonlinearities. Wang and Liu [38] researched the sliding mode control of the master-slave chaotic systems with sector nonlinear input. Yang et al. [39] addressed an adaptive two-stage sliding mode control to realize the synchronization for a class of n-dimensional nonlinear systems with sector nonlinearity input. Although the researches on sector nonlinear input have achieved certain results, most existing studies mainly focus on a single system rather than complex networks. Recently, Fang et al. [40] studied the modified function projective synchronization of complex dynamic networks with sector nonlinear input. In the controller design, it is assumed that the range of the sector nonlinear input is known. However, it is difficult to determine the exact boundary value of the sector nonlinear input. Once the restricted boundary of the control input is unknown, the controller designed in [40] is no longer applicable. How to realize function projective synchronization of complex dynamic networks under unknown sector nonlinear input is a challenging research topic.

Based on the results of previous researches, the function projective synchronization for a class of complex dynamic networks with unknown sector nonlinear input, multiple time-varying delay couplings, model uncertainty, and external interferences is studied in this paper. Through the designed adaptive controller, two complex dynamic networks can realize synchronization according to the corresponding function scaling factor. Compared with the existing research results, the contributions of this paper are (a) the complex network model includes the input nonlinearity, multiple time-varying delay couplings, model uncertainty, and external interferences, which is a more general model. (b) Many of the existing studies are concerned with synchronization between complex networks and single systems. This paper studies the synchronization between two complex networks, which is more complex and general. (c) Different from known sector nonlinear inputs in previous studies, this paper investigates the function projective synchronization of complex dynamic networks with unknown sector inputs. The boundary value of the sector nonlinear input and the delay term is not needed in controller design, so it is relatively easy to implement in practical engineering. (d) Function projective synchronization is a more general synchronization form. The controller in this paper can also realize complete synchronization, antisynchronization, and projective synchronization of complex dynamic networks.

2. Model Description

In this article, a type of complex dynamic networks with unknown sector nonlinear input, multiple time-varying delay couplings, model uncertainty, and external interferences is described as the drive system:

$$\begin{aligned}\dot{x}_i(t) &= f_i(x_i(t)) + F_i(x_i(t))\theta_i + \sum_{l=0}^{m-1} c_l(t) \sum_{j=1}^{N} a_{ij}^l \Gamma_l x_j(t-\tau_l(t)) + d_i^v(t) \\ &= f_i(x_i(t)) + F_i(x_i(t))\theta_i + c_0(t)\sum_{j=1}^{N} a_{ij}^0 \Gamma_0 x_j(t-\tau_0(t)) \\ &\quad + c_1(t)\sum_{j=1}^{N} a_{ij}^1 \Gamma_1 x_j(t-\tau_1(t)) + \cdots \\ &\quad + c_{m-1}(t)\sum_{j=1}^{N} a_{ij}^{m-1} \Gamma_{m-1} x_j(t-\tau_{m-1}(t)) + d_i^v(t),\end{aligned} \tag{1}$$

the corresponding response system is

$$\begin{aligned}\dot{y}_i(t) &= g_i(y_i(t)) + G_i(y_i(t))\eta_i + \sum_{l=0}^{m-1} c_l(t) \sum_{j=1}^{N} a_{ij}^l \Gamma_l y_j(t-\tau_l(t)) \\ &\quad + d_i^s(t) + \phi_i(u_i(t)) \\ &= g_i(y_i(t)) + G_i(y_i(t))\eta_i + c_0(t)\sum_{j=1}^{N} a_{ij}^0 \Gamma_0 y_j(t-\tau_0(t)) \\ &\quad + c_1(t)\sum_{j=1}^{N} a_{ij}^1 \Gamma_1 y_j(t-\tau_1(t)) + \cdots \\ &\quad + c_{m-1}(t)\sum_{j=1}^{N} a_{ij}^{m-1} \Gamma_{m-1} y_j(t-\tau_{m-1}(t)) + d_i^s(t) + \phi_i(u_i(t)),\end{aligned} \tag{2}$$

where $x_i(t) = (x_{i1}(t), x_{i2}(t), \cdots, x_{in}(t))^T$, $i = 1, 2, \cdots, N$ is the state vector of the ith node in the drive system, $y_i(t) = (y_{i1}(t), y_{i2}(t), \cdots, y_{in}(t))^T$, $i = 1, 2, \cdots, N$ is the state vector of the ith node in the response system. $f_i(\times), g_i(\times)\hat{I}R^n$ are the continuous nonlinear function vectors, R^n denotes the n

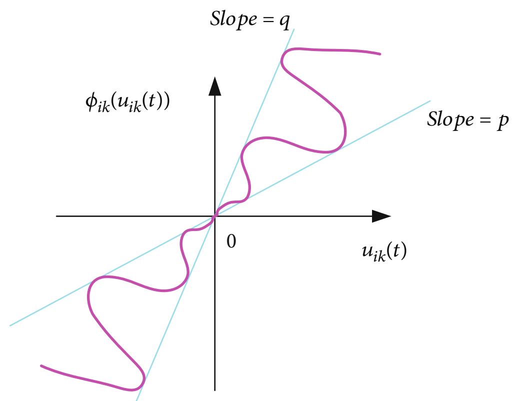

FIGURE 1: The nonlinear input $\phi_{ik}(u_{ik}(t))$ within the sector.

-dimensional vector space on the real number field R, $\theta_i, \eta_i \in R^w$ are unknown w-dimensional constant parameter vector, $F_i(\cdot), G_i(\cdot) \in R^{n\times w}$ are the continuous nonlinear function matrices, $R^{n\times w}$ denotes the $n\times w$ order matrix on the real number field R. $d_i^v(t)$ and $d_i^s(t)$ are the disturbances. The complex network is divided into subnetworks by $\tau_l(t)$, $\tau_l(t) \geq 0$, $(l = 0, 1, \cdots, m-1)$ is the different time-varying delays, and especially $\tau_0(t) = 0$ means that the coupling delay is 0; $c_l(t)$ is the coupling strength; Γ_l is the inner coupling matrix; $A_l = (a_{ij}^l)_{N\times N}$ is weight configuration matrix, representing the topological structure of the network. If nodes i and $j(j \neq i)$ are connected, then, $a_{ij}^l \neq 0$. If nodes i and $j(j\neq i)$ have no connection, then. $a_{ij}^l = a_{ji}^l = 0$. The diagonal elements of the matrix A_l are defined as $a_{ii}^l = -\sum_{j=1, j\neq i}^{N} a_{ij}^l$, $(i, j = 1, 2, \cdots, N)$. $\phi_i(u_i(t)) = [\phi_{i1}(u_{i1}(t)), \phi_{i2}(u_{i2}(t)), \cdots, \phi_{in}(u_{in}(t))]^{\mathrm{T}} (\phi_i(0) = 0)$ is the control input. $\phi_{ik}(u_{ik}(t))$ is in a sector $[pu_{ik}(t), qu_{ik}(t)]$, where p and q are two positive numbers and satisfy $p \leq \phi_{ik}(u_{ik}(t))/u_{ik}(t) \leq q$ when $u_{ik}(t) \neq 0$. The sector nonlinear input is shown in Figure 1.

Definition 1 (see [15]). For the complex dynamic networks (1) and (2), if Eq. (3) holds, the complex network (1) and (2) will realize function projective synchronization when

$$\lim_{t\longrightarrow\infty} \|e_i(t)\| = \lim_{t\longrightarrow\infty} \|y_i(t) - h(t)x_i(t)\| = 0, i = 1, 2, \cdots, N. \tag{3}$$

where $e_i(t) = (e_{i1}(t), e_{i2}(t), \cdots, e_{in}(t))^{\mathrm{T}}, i = 1, 2, \cdots, N$, $\|\cdot\|$ denotes the Euclidean norm of a vector. $h(t) \neq 0$ is function scaling factor, which is a continuously differentiable and bounded function.

Assumption 2. External disturbances $d_i^v(t)$ and $d_i^s(t)$ are bounded, and there exist positive constants α_i^v, α_i^s, such that $|d_i^v(t)| \leq \alpha_i^v$, $|d_i^s(t)| \leq \alpha_i^s$.

Corollary 3. *Because $h(t)$ is a continuously differentiable and bounded function, there exists a positive constant $\hbar$ and satisfies $|h(t)| \leq \hbar$. Under Assumption 2, there exists a positive constant $\alpha_i \geq \alpha_i^s + \hbar\alpha_i^w$, such that*

$$\begin{aligned} |d_i^s(t) - h(t)d_i^v(t)| &\leq |d_i^s(t)| + |h(t)d_i^v(t)| \\ &\leq |d_i^s(t) + |h(t)|||d_i^v(t)| \\ &\leq \alpha_i^s + \hbar\alpha_i^v \leq \alpha_i. \end{aligned} \tag{4}$$

Assumption 4. The time-varying coupling strength $c_l(t)$ is bounded, and there exists a positive constant c, such that

$$|c_l(t)| \leq c. \tag{5}$$

Assumption 5. The time-varying delay $\tau_l(t), l = 0, 1, \cdots, m-1$ is a continuously differentiable function and satisfies $0 \leq \dot{\tau}_l(t) \leq \varepsilon < 1$, so it is easy to get

$$\frac{1-\dot{\tau}_l(t)}{2(1-\varepsilon)} \geq \frac{1-\varepsilon}{2(1-\varepsilon)} = \frac{1}{2}, \tag{6}$$

where $0 < \varepsilon < 1$ is positive constant. This assumption is still satisfied if $\tau_l(t)$ is zero or some other constants.

Lemma 6 (see [9]). *For any vectors $X, Y \in R^n$ and a positive definite matrix $Q \in R^{n\times n}$ (R^n denotes the n-dimensional vector space on the real number field R, $R^{n\times n}$ denotes the $n\times n$ order matrix on the real number field R), the following matrix inequality holds:$2X^TQY \leq X^TQQ^TX + Y^TY$.*

Proof. Let $A = (a_1(t), a_2(t), \cdots, a_n(t))^{\mathrm{T}}, B = (b_1(t), b_2(t), \cdots, b_n(t))^{\mathrm{T}}$.

It is easy to get $A^{\mathrm{T}}B, B^{\mathrm{T}}A \in R$ and $A^{\mathrm{T}}B = B^{\mathrm{T}}A$, $A^{\mathrm{T}}A = a_1^2 + a_2^2 + \cdots + a_n^2$, $B^{\mathrm{T}}B = b_1^2 + b_2^2 + \cdots + b_n^2$, $A^{\mathrm{T}}B = B^{\mathrm{T}}A = a_1\times b_1 + a_2\times b_2 + \cdots + a_n\times b_n$.

Because $a_1^2 + a_2^2 + \cdots + a_n^2 + b_1^2 + b_2^2 + \cdots + b_n^2 - 2\times(a_1\times b_1 + a_2\times b_2 + \cdots + a_n\times b_n) = (a_1 - b_1)^2 + (a_2 - b_2)^2 + \cdots + (a_n - b_n)^2 \geq 0$,then, $a_1^2 + a_2^2 + \cdots + a_n^2 + b_1^2 + b_2^2 + \cdots + b_n^2 \geq 2\times(a_1\times b_1 + a_2\times b_2 + \cdots + a_n\times b_n)$, i.e., $A^{\mathrm{T}}A + B^{\mathrm{T}}B \geq 2A^{\mathrm{T}}B$.

Let $A = Q^{\mathrm{T}}X, B = Y$, then, we can get $2X^{\mathrm{T}}QY \leq X^{\mathrm{T}}QQ^{\mathrm{T}}X + Y^{\mathrm{T}}Y$.

This completes the proof. □

3. Controller Design

To realize function projective synchronization, the controller and parameter adaptive laws are designed as follows:

$$\begin{aligned} u_{ik}(t) = -\gamma\Bigg[\Bigg(&\left|g_{ik}(y_i(t)) - h(t)f_{ik}(x_i(t)) - \dot{h}(t)x_{ik}(t)\right| \\ &+ \left|G_{ik}(y_i(t))\widehat{\eta}_i - h(t)F_{ik}(x_i(t))\widehat{\theta}_i\right| + \frac{1}{\gamma}\widehat{\nu}|e_{ik}(t)|\Bigg)\widehat{\omega} \\ &+ \widehat{\psi}_{ik}\Bigg] \operatorname{sgn}(e_{ik}(t)), i = 1, 2, \cdots, N\, k = 1, 2, \cdots, n. \end{aligned} \tag{7}$$

$$\dot{\widehat{\theta}}_i = -F_i^{\mathrm{T}}(x_i(t))h(t)e_i(t), \tag{8}$$

$$\dot{\widehat{\eta}}_i = G_i^{\mathrm{T}}(y_i(t))e_i(t), \tag{9}$$

$$\begin{aligned}\dot{\hat{\varpi}} = \sum_{i=1}^{N}\left|e_i^{\mathrm{T}}(t)\right|\Big[\left|g_i(y_i(t)) - h(t)f_i(x_i(t)) - \dot{h}(t)x_i(t)\right| \\ + \left|G_i(y_i(t))\hat{\eta}_i - h(t)F_i(x_i(t))\hat{\theta}_i\right| + \hat{\nu}e_i(t)\Big],\end{aligned} \tag{10}$$

$$\dot{\hat{\psi}}_i = |e_i(t)|, \tag{11}$$

$$\dot{\hat{\nu}} = \sum_{i=1}^{N} e_i^{\mathrm{T}}(t)e_i(t), \tag{12}$$

where γ, ν are positive constants and satisfy $\gamma > 1, \nu > 0. \varpi = 1/p > 0, \psi_i = \alpha_i/p > 0. \hat{\varpi}, \hat{\psi}_i, \hat{\theta}_i, \hat{\eta}_i, \hat{\nu}$ is the estimated parameter for $\varpi, \psi_i, \theta_i, \eta_i, \nu$, respectively. $F_{ik}(\cdot), G_{ik}(\cdot) \in R^{1\times w}$ are the kth row of the function matrices $F_i(\cdot), G_i(\cdot) \in R^{n\times w}$.

Remark 7. Let $u_{ik}(t) = -\gamma\mu_{ik}\,\mathrm{sgn}\,(e_{ik}(t))$, then, $\mu_{ik} = (|g_{ik}(y_i(t)) - h(t)f_{ik}(x_i(t)) - \dot{h}(t)x_{ik}(t)| + |G_{ik}(y_i(t))\hat{\eta}_i - h(t)F_{ik}(x_i(t))\hat{\theta}_i| + (1/\gamma)\hat{\nu}|e_{ik}(t)|)\hat{\varpi} + \hat{\psi}_{ik}$.

Because $\gamma > 1, \nu > 0, \varpi = 1/p > 0, \psi_i = \alpha_i/p > 0$, we can get $\mu_{ik} > 0$.

Lemma 8 (see [40]). *Let $u_{ik}(t) = -\gamma\mu_{ik}\,\mathrm{sgn}\,(e_{ik}(t)), \mu_{ik} > 0$, we can get $\sum_{i=1}^{N} e_{ik}(t)\phi_{ik}(u_{ik}(t)) \le \sum_{i=1}^{N} -p\gamma\mu_{ik}|e_{ik}(t)|$, i.e., $e_i^T(t)\phi_i(u_i(t)) \le -p_i\gamma{\mu_i}^T|e_i(t)|$.*

Proof. It can be known from $p \le \phi_{ik}(u_{ik}(t))/u_{ik}(t) \le q$ that $pu_{ik}^2(t) \le u_{ik}(t)\phi_{ik}(u_{ik}(t)) \le qu_{ik}^2(t)$.

When $e_{ik}(t) = 0$, the equation obviously holds, that is, $e_{ik}(t)\phi_{ik}(u_{ik}(t)) = -p\gamma\mu_{ik}|e_{ik}(t)|$.

When $e_{ik}(t) \ne 0$, substituting $u_{ik}(t) = -\gamma\mu_{ik}\,\mathrm{sgn}\,(e_{ik}(t))$ into $pu_{ik}^2(t) \le u_{ik}(t)\phi_{ik}(u_{ik}(t)) \le qu_{ik}^2(t)$, we can get $p\gamma^2\mu_{ik}^2\,\mathrm{sgn}^2(e_{ik}(t)) \le -\gamma\mu_{ik}\,\mathrm{sgn}\,(e_{ik}(t))\phi_{ik}(u_{ik}(t))$.

Using $|e_{ik}(t)|/e_{ik}(t)$ instead of sgn $(e_{ik}(t))$, we can get $p\gamma^2\mu_{ik}^2|e_{ik}(t)||e_{ik}(t)|/e_{ik}(t)e_{ik}(t) \le -\gamma\mu_{ik}\phi_{ik}(\mu_{ik}(t))|e_{ik}(t)|/e_{ik}(t)$.

Multiplying both sides of the inequality by ${e_{ik}}^2(t)$, we can get $p\gamma^2\mu_{ik}^2|e_{ik}(t)|^2 \le -\gamma\mu_{ik}|e_{ik}(t)|e_{ik}(t)\phi_{ik}(u_{ik}(t))$. Dividing both sides by $\gamma\mu_{ik}|e_{ik}(t)|$, we can get $e_{ik}(t)\phi_{ik}(u_{ik}(t)) \le -p\gamma\mu_{ik}|e_{ik}(t)|$.

It is easy to get $\sum_{i=1}^{N} e_{ik}(t)\phi_{ik}(u_{ik}(t)) \le \sum_{i=1}^{N} -p\gamma\mu_{ik}|e_{ik}(t)|$, then, $e_i^{\mathrm{T}}(t)\phi_i(u_i(t)) \le -p_i\gamma{\mu_i}^{\mathrm{T}}|e_i(t)|$.

This completes the proof. □

Theorem 9. *If Assumptions 2–5 are satisfied, the drive system (1) and the response system (2) can realize function projective synchronization with the controller (7) and adaptive laws (8)–(12).*

Proof. From Definition 1, we have the error term:

$$e_i(t) = y_i(t) - h(t)x_i(t). \tag{13}$$

The time derivative of $e_i(t)$ is

$$\begin{aligned}\dot{e}_i(t) &= \dot{y}_i(t) - h(t)\dot{x}_i(t) - \dot{h}(t)x_i(t) \\ &= g_i(y_i(t)) + G_i(y_i(t))\eta_i + \sum_{l=0}^{m-1} c_l(t)\sum_{j=1}^{N} a_{ij}^l\Gamma_l y_j(t-\tau_l(t)) \\ &\quad + d_i^s(t) + \phi_i(u_i(t)) - h(t)f_i(x_i(t)) - h(t)F_i(x_i(t))\theta_i \\ &\quad - h(t)\sum_{l=0}^{m-1} c_l(t)\sum_{j=1}^{N} a_{ij}^l\Gamma_l x_j(t-\tau_l(t)) \\ &\quad - h(t)d_i^v(t) - \dot{h}(t)x_i(t).\end{aligned} \tag{14}$$

Choosing Lyapunov function as

$$\begin{aligned}V(t) &= \frac{1}{2p}\sum_{i=1}^{N}\left[e_i^{\mathrm{T}}(t)e_i(t) + p\left(\hat{\psi}_i - \psi_i\right)^2\right] \\ &\quad + \frac{1}{2}\left(\hat{\varpi} - \varpi\right)^2 + \frac{1}{2p}\left(\hat{\nu} - \nu^*\right)^2 \\ &\quad + \frac{1}{2p}\left[\sum_{i=1}^{N}\left(\hat{\theta}_i - \theta_i\right)^2 + \sum_{i=1}^{N}\left(\hat{\eta}_i - \eta_i\right)^2\right. \\ &\quad \left. + \frac{1}{(1-\varepsilon)}\int_{t-\tau_l(t)}^{t}\sum_{l=1}^{m-1}\sum_{i=1}^{N} e_i^{\mathrm{T}}(\delta)e_i(\delta)d\delta\right],\end{aligned} \tag{15}$$

where $\hat{\varpi}, \hat{\psi}_i$ is the estimated parameter for ϖ, ψ_i. ν^* is the positive constant to be designed.

Taking the derivative of the Lyapunov function, we can get

$$\begin{aligned}\dot{V}(t) &= \sum_{i=1}^{N}\left[\frac{1}{p}e_i^{\mathrm{T}}(t)\dot{e}_i(t) + \left(\hat{\psi}_i - \psi_i\right)^{\mathrm{T}}\dot{\hat{\psi}}_i\right] + \left(\hat{\varpi} - \varpi\right)\dot{\hat{\varpi}} \\ &\quad + \frac{1}{p}\left(\hat{\nu} - \nu^*\right)\dot{\hat{\nu}} + \frac{1}{p}\sum_{i=1}^{N}\left(\hat{\theta}_i - \theta_i\right)^{\mathrm{T}}\dot{\hat{\theta}}_i \\ &\quad + \frac{1}{p}\sum_{i=1}^{N}\left(\hat{\eta}_i - \eta_i\right)^{\mathrm{T}}\dot{\hat{\eta}}_i + \frac{\sum_{l=1}^{m-1}\sum_{i=1}^{N} e_i^{\mathrm{T}}(t)e_i(t)}{2p(1-\varepsilon)} \\ &\quad - \frac{1-\dot{\tau}_l(t)}{2p(1-\varepsilon)}\sum_{l=1}^{m-1}\sum_{i=1}^{N} e_i^{\mathrm{T}}(t-\tau_l(t))e_i(t-\tau_l(t)).\end{aligned} \tag{16}$$

Substituting (8), (9), and (14) into (16), we can get

$$\begin{aligned}\dot{V}(t) &= \frac{1}{p}\sum_{i=1}^{N}\Big[e_i^{\mathrm{T}}(t)(g_i(y_i(t)) + G_i(y_i(t))\eta_i + d_i^s(t) \\ &\quad + \sum_{l=0}^{m-1} c_l(t)\sum_{j=1}^{N} a_{ij}^l\Gamma_l y_j(t-\tau_l(t)) + \phi_i(u_i(t)) \\ &\quad - h(t)f_i(x_i(t)) - h(t)F_i(x_i(t))\theta_i - h(t)\sum_{l=0}^{m-1} \\ &\quad \cdot c_l(t)\sum_{j=1}^{N} a_{ij}^l\Gamma_l x_j(t-\tau_l(t)) - h(t)d_i^v(t) - \dot{h}(t)x_i(t)\Big)\Big]\end{aligned}$$

$$+\sum_{i=1}^{N}\left[\left(\widehat{\psi}_i-\psi_i\right)^{\mathrm{T}}\dot{\widehat{\psi}}_i\right]+\left(\widehat{\varpi}-\varpi\right)\dot{\widehat{\varpi}}+\frac{1}{p}\left(\widehat{\nu}-\nu^*\right)\dot{\widehat{\nu}}$$
$$-\frac{1}{p}\sum_{i=1}^{N}\left(\widehat{\theta}_i-\theta_i\right)^{\mathrm{T}}F_i^{\mathrm{T}}(x_i(t))h(t)e_i(t)$$
$$+\frac{1}{p}\sum_{i=1}^{N}\left(\widehat{\eta}_i-\eta_i\right)^{\mathrm{T}}G_i^{\mathrm{T}}(y_i(t))e_i(t)$$
$$+\frac{1}{2p(1-\varepsilon)}\sum_{l=1}^{m-1}\sum_{i=1}^{N}e_i^{\mathrm{T}}(t)e_i(t)$$
$$-\frac{1-\dot{\tau}_l(t)}{2p(1-\varepsilon)}\sum_{l=1}^{m-1}\sum_{i=1}^{N}e_i^{\mathrm{T}}(t-\tau_l(t))e_i(t-\tau_l(t)). \tag{17}$$

Because $\sum_{i=1}^{N}e_i^{\mathrm{T}}(t)h(t)F_i(x_i(t))\theta_i=\sum_{i=1}^{N}\theta_i^{\mathrm{T}}F_i^{\mathrm{T}}(x_i(t))h(t)e_i(t),\sum_{i=1}^{N}e_i^{\mathrm{T}}(t)G_i(y_i(t))\eta_i=\sum_{i=1}^{N}\eta^{\mathrm{T}}G_i^{T}(y_i(t))e_i(t)$, we can get

$$-\frac{1}{p}\sum_{i=1}^{N}e_i^{\mathrm{T}}(t)h(t)F_i(x_i(t))\theta_i$$
$$-\frac{1}{p}\sum_{i=1}^{N}\left(\widehat{\theta}_i-\theta_i\right)^{\mathrm{T}}F_i^{\mathrm{T}}(x_i(t))h(t)e_i(t) \tag{18}$$
$$=-\frac{1}{p}\sum_{i=1}^{N}\widehat{\theta}_i^{\mathrm{T}}F_i^{\mathrm{T}}(x_i(t))h(t)e_i(t),$$

$$\frac{1}{p}\sum_{i=1}^{N}e_i^{\mathrm{T}}(t)G_i(y_i(t))\eta_i+\frac{1}{p}\sum_{i=1}^{N}\left(\widehat{\eta}_i-\eta_i\right)^{\mathrm{T}}G_i^{\mathrm{T}}(y_i(t))e_i(t)$$
$$=\frac{1}{p}\sum_{i=1}^{N}\widehat{\eta}_i^{\mathrm{T}}G_i^{\mathrm{T}}(y_i(t))e_i(t), \tag{19}$$

so

$$\dot{V}(t)=\frac{1}{p}\sum_{i=1}^{N}\Big[e_i^{\mathrm{T}}(t)\Big(g_i(y_i(t))+\sum_{l=0}^{m-1}c_l(t)\sum_{j=1}^{N}a_{ij}^{l}\Gamma_l y_j(t-\tau_l(t))$$
$$+\phi_i(u_i(t))+d_i^{s}(t)-h(t)f_i(x_i(t))-h(t)\sum_{l=0}^{m-1}c_l(t)$$
$$\cdot\sum_{j=1}^{N}a_{ij}^{l}\Gamma_l x_j(t-\tau_l(t))-h(t)d_i^{w}(t)-\dot{h}(t)x_i(t)\Big)\Big]$$
$$+\sum_{i=1}^{N}\left[\left(\widehat{\psi}_i-\psi_i\right)^{\mathrm{T}}\dot{\widehat{\psi}}_i\right]+\left(\widehat{\varpi}-\varpi\right)\dot{\widehat{\varpi}}$$
$$-\frac{1}{p}\sum_{i=1}^{N}\widehat{\theta}_i^{\mathrm{T}}F_i^{\mathrm{T}}(x_i(t))h(t)e_i(t)+\frac{1}{p}\sum_{i=1}^{N}\widehat{\eta}_i^{\mathrm{T}}G_i^{\mathrm{T}}(y_i(t))e_i(t)$$
$$+\frac{1}{p}\left(\widehat{\nu}-\nu^*\right)\dot{\widehat{\nu}}+\frac{1}{2p(1-\varepsilon)}\sum_{l=1}^{m-1}\sum_{i=1}^{N}e_i^{\mathrm{T}}(t)e_i(t)$$
$$-\frac{1-\dot{\tau}_l(t)}{2p(1-\varepsilon)}\sum_{l=1}^{m-1}\sum_{i=1}^{N}e_i^{\mathrm{T}}(t-\tau_l(t))e_i(t-\tau_l(t)). \tag{20}$$

Substituting Lemma 8 and Corollary 3 into (20), we can get

$$\dot{V}(t)\le\frac{1}{p}\sum_{i=1}^{N}\Big[\left|e_i^{\mathrm{T}}(t)\right|\left(\left|g_i(y_i(t))-h(t)f_i(x_i(t))-\dot{h}(t)x_i(t)\right|+\alpha_i\right)$$
$$-\gamma\mu_i^{\mathrm{T}}|e_i(t)|\Big]+\sum_{i=1}^{N}\left[\left(\widehat{\psi}_i-\psi_i\right)^{\mathrm{T}}\dot{\widehat{\psi}}_i\right]+\left(\widehat{\varpi}-\varpi\right)\dot{\widehat{\varpi}}$$
$$-\frac{1}{p}\sum_{i=1}^{N}\widehat{\theta}_i^{\mathrm{T}}F_i^{\mathrm{T}}(x_i(t))h(t)e_i(t)+\frac{1}{p}\sum_{i=1}^{N}\widehat{\eta}_i^{\mathrm{T}}G_i^{\mathrm{T}}(y_i(t))e_i(t)$$
$$+\frac{1}{p}\left(\widehat{\nu}-\nu^*\right)\dot{\widehat{\nu}}+\frac{1}{p}\sum_{i=1}^{N}\Big[e_i^{\mathrm{T}}(t)\Big(c_l\sum_{j=1}^{N}a_{ij}^{0}\Gamma_0 e_j(t)$$
$$+c_l\sum_{l=1}^{m-1}\sum_{j=1}^{N}a_{ij}^{l}\Gamma_l e_j(t-\tau_l(t))\Big]+\frac{1}{2p(1-\varepsilon)}\sum_{l=1}^{m-1}\sum_{i=1}^{N}$$
$$\cdot e_i^{\mathrm{T}}(t)e_i(t)-\frac{1-\dot{\tau}_l(t)}{2p(1-\varepsilon)}\sum_{l=1}^{m-1}\sum_{i=1}^{N}e_i^{\mathrm{T}}(t-\tau_l(t))e_i(t-\tau_l(t)). \tag{21}$$

Substituting $\psi_i=\alpha_i/p$ and $\varpi=1/p$ into (21), because $\widehat{\eta}_i^{\mathrm{T}}G_i^{\mathrm{T}}(y_i)e_i-\widehat{\theta}_i^{\mathrm{T}}F_i^{\mathrm{T}}(x_i)he_i=(\widehat{\eta}_i^{\mathrm{T}}G_i^{\mathrm{T}}(y_i)-\widehat{\theta}_i^{\mathrm{T}}F_i^{\mathrm{T}}(x_i)h)e_i\le|\widehat{\eta}_i^{\mathrm{T}}G_i^{\mathrm{T}}(y_i)-\widehat{\theta}_i^{\mathrm{T}}F_i^{\mathrm{T}}(x_i)h||e_i|=|\widehat{\eta}_i^{\mathrm{T}}G_i^{\mathrm{T}}(y_i)|e_i|-\widehat{\theta}_i^{\mathrm{T}}F_i^{\mathrm{T}}(x_i)h|e_i||$,where $|e_i|=(|e_{i1}|,|e_{i2}|,\cdots,|e_{in}|)^{\mathrm{T}}$, we can get

$$\dot{V}(t)\le\sum_{i=1}^{N}\Big[\varpi\left|e_i^{\mathrm{T}}(t)\right|\left|g_i(y_i(t))-h(t)f_i(x_i(t))-\dot{h}(t)x_i(t)\right|$$
$$+\left|e_i^{\mathrm{T}}(t)\right|\psi_i-\gamma\mu_i^{\mathrm{T}}|e_i(t)|+\left(\widehat{\psi}_i-\psi_i\right)^{\mathrm{T}}|e_i(t)|\Big]$$
$$+\left(\widehat{\varpi}-\varpi\right)\dot{\widehat{\varpi}}+\varpi_i\sum_{i=1}^{N}\left|\widehat{\eta}_i^{\mathrm{T}}G_i^{\mathrm{T}}(y_i)|e_i|-\widehat{\theta}_i^{\mathrm{T}}F_i^{\mathrm{T}}(x_i)h|e_i|\right|$$
$$+\varpi\left(\widehat{\nu}-\nu^*\right)\dot{\widehat{\nu}}+\sum_{i=1}^{N}\Big[\varpi_i e_i^{\mathrm{T}}(t)\Big(c_l\sum_{j=1}^{N}a_{ij}^{0}\Gamma_0 e_j(t)$$
$$+c_l\sum_{l=1}^{m-1}\sum_{j=1}^{N}a_{ij}^{l}\Gamma_l e_j(t-\tau_l(t))\Big)+\frac{\varpi_i}{2(1-\varepsilon)}$$
$$\cdot\sum_{l=1}^{m-1}\sum_{i=1}^{N}e_i^{\mathrm{T}}(t)e_i(t)-\frac{1-\dot{\tau}_l(t)}{2(1-\varepsilon)}$$
$$\cdot\varpi_i\sum_{l=1}^{m-1}\sum_{i=1}^{N}e_i^{\mathrm{T}}(t-\tau_l(t))e_i(t-\tau_l(t)). \tag{22}$$

Substituting (10) and (11) into (22), because $\sum_{i=1}^{N}|e^{\mathrm{T}}{}_i(t)|hF_i(x)\widehat{\theta}_i=\widehat{\theta}^{\mathrm{T}}F^{\mathrm{T}}(x)h|e|,\sum_{i=1}^{N}|e^{\mathrm{T}}{}_i(t)|G_i(y)\widehat{\eta}_i=\widehat{\eta}^{\mathrm{T}}G^{\mathrm{T}}(y)|e|$, then, the above formula can be simplified as

$$\begin{aligned}\dot{V}(t)\le&\sum_{i=1}^{N}\left[\left|e_i^{\mathrm{T}}(t)\right|\psi_i-\gamma\left|e_i^{\mathrm{T}}(t)\right|\left[\left(\left(|g_i(y_i(t))-h(t)f_i(x_i(t))\right.\right.\right.\right.\\&\left.-\dot{h}(t)x_i(t)\right|+\left|G_i(y)\widehat{\eta}_i-h(t)F_i(x)\widehat{\theta}_i\right|\\&\left.\left.+\frac{1}{\gamma}\widehat{\nu}e_i(t)\right)\widehat{\omega}+\widehat{\psi}_i\right]+\left(\widehat{\psi}_i-\psi_i\right)^{\mathrm{T}}|e_i(t)|\Big]\\&+\widehat{\omega}\sum_{i=1}^{N}\left|e_i^{\mathrm{T}}(t)\right|\left[\left|g_i(y_i(t))-h(t)f_i(x_i(t))-\dot{h}(t)x_i(t)\right|\right.\\&\left.+\left|G_i(y)\widehat{\eta}_i-h(t)F_i(x)\widehat{\theta}_i\right|\right]+\sum_{i=1}^{N}\left[\varpi e_i^{\mathrm{T}}(t)(c_l\sum_{j=1}^{N}a_{ij}^0\Gamma_0e_j\right.\\&\left.\cdot(t)+c_l\sum_{l=1}^{m-1}\sum_{j=1}^{N}a_{ij}^l\Gamma_le_j(t-\tau_l(t))\right]-\varpi\nu^*\sum_{i=1}^{N}e_i^{\mathrm{T}}(t)e_i(t)\\&+\frac{\varpi}{2(1-\varepsilon)}\sum_{l=1}^{m-1}\sum_{i=1}^{N}e_i^{\mathrm{T}}(t)e_i(t)-\frac{1-\dot{\tau}_l(t)}{2(1-\varepsilon)}\\&\cdot\varpi\sum_{l=1}^{m-1}\sum_{i=1}^{N}e_i^{\mathrm{T}}(t-\tau_l(t))e_i(t-\tau_l(t)).\end{aligned}\tag{23}$$

In order to simplify the proof process, $\dot{V}(t)$ is decomposed into two parts $\dot{V}_1(t)$ and $\dot{V}_2(t)$:

$$\begin{aligned}\dot{V}_1(t)=&\sum_{i=1}^{N}\left[\frac{1}{p}e_i^{\mathrm{T}}(t)\left(c_l\sum_{j=1}^{N}a_{ij}^0\Gamma_0e_j(t)\right.\right.\\&\left.+c_l\sum_{l=1}^{m-1}\sum_{j=1}^{N}a_{ij}^l\Gamma_le_j(t-\tau_l(t))\right)\\&+\frac{1}{2p(1-\varepsilon)}\sum_{l=1}^{m-1}\sum_{i=1}^{N}e_i^{\mathrm{T}}(t)e_i(t)\\&-\frac{1-\dot{\tau}_l(t)}{2p(1-\varepsilon)}\sum_{l=1}^{m-1}\sum_{i=1}^{N}e_i^{\mathrm{T}}(t-\tau_l(t))e_i(t-\tau_l(t))\\&-\frac{\nu^*}{p}\sum_{i=1}^{N}e_i^{\mathrm{T}}(t)e_i(t),\end{aligned}\tag{24}$$

$$\begin{aligned}\dot{V}_2(t)=&\sum_{i=1}^{N}\left[\left|e_i^{\mathrm{T}}(t)\right|\psi_i-\gamma\left|e_i^{\mathrm{T}}(t)\right|\left[\left(\left(|g_i(y_i(t))-h(t)f_i(x_i(t))\right.\right.\right.\right.\\&\left.\left.-\dot{h}(t)x_i(t)\right|+\left|G_i(y)\widehat{\eta}_i-h(t)F_i(x)\widehat{\theta}_i\right|\right)\widehat{\omega}+\widehat{\psi}_i\Big]\\&\left.+\widehat{\psi}_i^{\mathrm{T}}|e_i(t)|\right]+\widehat{\omega}\sum_{i=1}^{N}\left|e_i^{\mathrm{T}}(t)\right|\left[\left|g_i(y_i(t))-h(t)f_i(x_i(t))\right.\right.\\&\left.\left.-\dot{h}(t)x_i(t)\right|+\left|G_i(y)\widehat{\eta}_i-h(t)F_i(x)\widehat{\theta}_i\right|\right].\end{aligned}\tag{25}$$

Let $e(t)=(e_1^T(t),e_2^T(t),\cdots,e_N^T(t))^T\in R^{N\times 1}$, $B_0=(A_0\otimes\Gamma_0)$, $B_1=(A_1\otimes\Gamma_1),\cdots,B_l=(A_l\otimes\Gamma_l)$, where $\otimes$ represents the Kronecker product, then, we can get

$$\begin{aligned}\dot{V}_1(t)\le&\frac{1}{p}\left(c_le^{\mathrm{T}}(t)B_0e(t)+c_l\sum_{l=1}^{m-1}e^{\mathrm{T}}(t)B_le(t-\tau_l(t))\right.\\&+\frac{1}{2(1-\varepsilon)}\sum_{l=1}^{m-1}e^{\mathrm{T}}(t)e(t)-\frac{1}{2}\sum_{l=1}^{m-1}e^{\mathrm{T}}(t-\tau_l(t))\\&\left.\cdot e(t-\tau_l(t))-\nu^*e^{\mathrm{T}}(t)e(t)\right).\end{aligned}\tag{26}$$

Based on Lemma 6, it is

$$\begin{aligned}c_le^{\mathrm{T}}(t)B_le(t-\tau_l(t))\le&\frac{1}{2}c_l^2e^{\mathrm{T}}(t)B_lB_l^{\mathrm{T}}e(t)\\&+\frac{1}{2}e^{\mathrm{T}}(t-\tau_l(t))e(t-\tau_l(t)),\end{aligned}\tag{27}$$

so we can get

$$\begin{aligned}\dot{V}_1(t)\le&\frac{1}{p}\left(e^{\mathrm{T}}(t)\left[c_lB_0+\frac{1}{2}c_l^2\sum_{l=1}^{m-1}B_lB_l^{\mathrm{T}}\right]e(t)\right.\\&\left.+\sum_{l=1}^{m-1}\frac{1}{2(1-\varepsilon)}e^{\mathrm{T}}(t)e(t)-\nu^*e^{\mathrm{T}}(t)e(t)\right)\\\le&\frac{1}{p}\left([\lambda_{\max}\left(c_lB_0+\frac{1}{2}c_l^2\sum_{l=1}^{m-1}B_lB_l^{\mathrm{T}}\right)\right.\\&\left.+\frac{m-1}{2(1-\varepsilon)}-\nu^*]e^{\mathrm{T}}(t)e(t)\right).\end{aligned}\tag{28}$$

Because $p>0$, if $\nu^*\ge\lambda_{\max}(c_lB_0+1/2c_l^2\sum_{l=1}^{m-1}B_lB_l^{\mathrm{T}})+m-1/2(1-\varepsilon)$, we can get $\dot{V}_1(t)\le 0$, where $\lambda_{\max}(Q)$ is the maximum eigenvalue of the matrix Q.

Making a simple equation transformation to $\dot{V}_2(t)$, we can get

$$\begin{aligned}\dot{V}_2(t)\le&\sum_{i=1}^{N}(1-\gamma)\left|e_i^{\mathrm{T}}(t)\right|\left[\left(\left(|g_i(y_i(t))-h(t)f_i(x_i(t))\right.\right.\right.\\&\left.\left.-\dot{h}(t)x_i(t)\right|+\left|G_i(y)\widehat{\eta}_i-h(t)F_i(x)\widehat{\theta}_i\right|\right)\widehat{\omega}+\widehat{\psi}_i\Big]\\\le&\sum_{i=1}^{N}(1-\gamma)\left|e_i^{\mathrm{T}}(t)\right|\mu_i.\end{aligned}\tag{29}$$

Because $\gamma>1,\varpi=1/p>0,\psi_i=\alpha_i/p>0$, then

$$\dot{V}_2(t)\le\sum_{i=1}^{N}(1-\gamma)\left|e_i^{\mathrm{T}}(t)\right|\mu_i\le 0.\tag{30}$$

Based on the above analysis, we can get that $\dot{V}(t)\le\dot{V}_1(t)+\dot{V}_2(t)\le 0$ if $\nu^*\ge\lambda_{\max}(c_lB_0+1/2c_l^2\sum_{l=1}^{m-1}B_lB_l^{\mathrm{T}})+m-1/2(1-\varepsilon)$. According to Lyapunov stability theory, we can obtain $e_i(t)\longrightarrow 0$ as $t\longrightarrow\infty$, which means that the function projective synchronization between the drive system (1) and the response system (2) is achieved. This completes the proof. □

Remark 10. In the proof of Theorem 9, based on Lyapunov stability theory and inequality transformation method, by introducing Lemma 6 and 8 and some reasonable Assumptions, the controller is designed flexibly without the boundary value (p and q) of the sector nonlinear input and the delay term $\tau_l(t)$.

Remark 11. When $\tau_l(t), l = 0, 1, 2, \cdots, m-1$ is constant or $\tau_0(t) = \tau_1(t) = \cdots = \tau_{m-1}(t) = \tau(t)$, the multiple time-varying delay couplings are transformed into constant time-delay coupling or single time-varying delay coupling. When $\tau_l(t), l = 0, 1, \cdots, m-1$ is constant or $\tau_0(t) = \tau_1(t) = \cdots = \tau_{m-1}(t) = \tau(t)$, Assumption 5 is also satisfied, and the control method in this article is also applicable to constant time-delay coupling or single time-varying delay coupling.

Remark 12. If $h(t)$ is a constant, the function projection synchronization is transformed into the projection synchronization. In particular, when $h(t) = 1$ or $h(t) = -1$, the function projection synchronization turns into complete synchronization or antisynchronization.

4. Numerical Simulation

In order to verify the correctness of the theoretical analysis, we select communication network with chaotic nodes as simulation examples.

$$\begin{aligned}
\begin{bmatrix} \dot{x}_{i1}(t) \\ \dot{x}_{i2}(t) \\ \dot{x}_{i3}(t) \end{bmatrix} &= \begin{bmatrix} 0 \\ -x_{i1}(t)x_{i3}(t) - x_{i2}(t) \\ x_{i1}(t)x_{i2}(t) \end{bmatrix} \\
&\quad + \begin{bmatrix} -x_{i1}(t) + x_{i2}(t) & 0 & 0 \\ 0 & x_{i1}(t) & 0 \\ 0 & 0 & -x_{i3}(t) \end{bmatrix} \\
&\quad \times \begin{bmatrix} \theta_{i1} \\ \theta_{i2} \\ \theta_{i3} \end{bmatrix} + \begin{bmatrix} d^v_{i1}(t) \\ d^v_{i2}(t) \\ d^v_{i3}(t) \end{bmatrix} + c_0(t)\sum_{j=1}^{4} a^0_{ij}\Gamma_0 x_j(t) \\
&\quad + c_1(t)\sum_{j=1}^{4} a^1_{ij}\Gamma_1 x_j(t-\tau_1(t)) \\
&\quad + c_2(t)\sum_{j=1}^{4} a^2_{ij}\Gamma_2 x_j(t-\tau_2(t)). \quad i = 1, 2, 3, 4.
\end{aligned} \tag{31}$$

Example 1. Considering a communication network with $N = 4$, $n = 3$, the drive system is composed of four Lorenz chaotic systems with two different time-varying delay couplings.

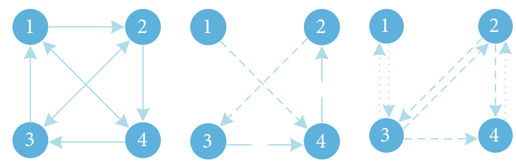

(a) $A0$ (b) $A1$ (c) $A2$

Figure 2: Topology of the multilink complex networks in Example 1 with four nodes and three subnetworks.

The response system is composed of four Chen chaotic systems with two different time-varying delay couplings.

$$\begin{aligned}
\begin{bmatrix} \dot{y}_{i1}(t) \\ \dot{y}_{i2}(t) \\ \dot{y}_{i3}(t) \end{bmatrix} &= \begin{bmatrix} 0 \\ -y_{i1}(t)y_{i3}(t) \\ y_{i1}(t)y_{i2}(t) \end{bmatrix} + \begin{bmatrix} y_{i2}(t) - y_{i1}(t) & 0 & 0 \\ -y_{i1}(t) & y_{i2}(t) + y_{i1}(t) & 0 \\ 0 & 0 & -y_{i3}(t) \end{bmatrix} \\
&\quad \times \begin{bmatrix} \eta_{i1} \\ \eta_{i2} \\ \eta_{i3} \end{bmatrix} + \begin{bmatrix} d^s_{i1}(t) \\ d^s_{i2}(t) \\ d^s_{i3}(t) \end{bmatrix} + \begin{bmatrix} \phi_{i1}(u_{i1}(t)) \\ \phi_{i2}(u_{i2}(t)) \\ \phi_{i3}(u_{i3}(t)) \end{bmatrix} \\
&\quad + c_0(t)\sum_{j=1}^{4} a^0_{ij}\Gamma_0 y_j(t) + c_1(t)\sum_{j=1}^{4} a^1_{ij}\Gamma_1 y_j(t-\tau_1(t)) \\
&\quad + c_2(t)\sum_{j=1}^{4} a^2_{ij}\Gamma_2 y_j(t-\tau_2(t)) . i = 1, 2, 3, 4.
\end{aligned} \tag{32}$$

In MATLAB numerical simulation, set $c_0 = c_1 = c_2 = 0.2$, $\tau_1(t) = t/3 + t$, $\tau_2(t) = e^t/3 + e^t$, $d_i(t) = 0.2 \cos t$, $\Gamma_0 = \Gamma_1 = \Gamma_2 = I^{3\times 3}$, $h(t) = 2 \cos 2t$. The nonlinear input is $\phi_i(u_i(t)) = [\phi_{i1}(u_{i1}(t)), \phi_{i2}(u_{i2}(t)), \phi_{i3}(u_{i3}(t))]^T = [(0.3 + 0.2 \cos (u_{i1}(t)))u_{i1}(t), (0.6 + 0.2 \sin (u_{i2}(t)))u_{i2}(t), (0.4 - 0.2 \cos (u_{i3}(t)))u_{i3}(t)]^T$. The topological structure matrices A_0, A_1, A_2 are as follows:

$$\begin{aligned}
A_0 &= \begin{pmatrix} -2 & 1 & 0 & 1 \\ 0 & -2 & 1 & 1 \\ 1 & 1 & -2 & 0 \\ 1 & 0 & 1 & -2 \end{pmatrix}, \\
A_1 &= \begin{pmatrix} -1 & 0 & 0 & 1 \\ 0 & -1 & 1 & 0 \\ 0 & 0 & -1 & 1 \\ 0 & 1 & 0 & -1 \end{pmatrix}, \\
A_2 &= \begin{pmatrix} -1 & 0 & 1 & 0 \\ 0 & -2 & 1 & 1 \\ 1 & 1 & -2 & 0 \\ 0 & 1 & 0 & -1 \end{pmatrix}.
\end{aligned} \tag{33}$$

And the topology of the driver network and response network is shown in Figure 2.

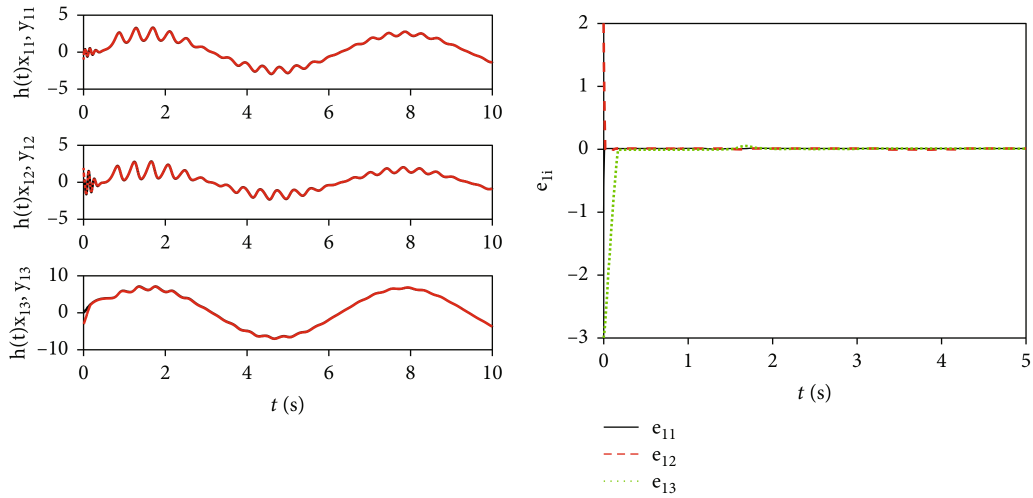

(a) Synchronization states $y_{1i}, h(t)x_{1i}$

(b) Synchronization errors e_{1i}

FIGURE 3: The time evolution of synchronization between y_{1i} and $h(t)x_{1i}$.

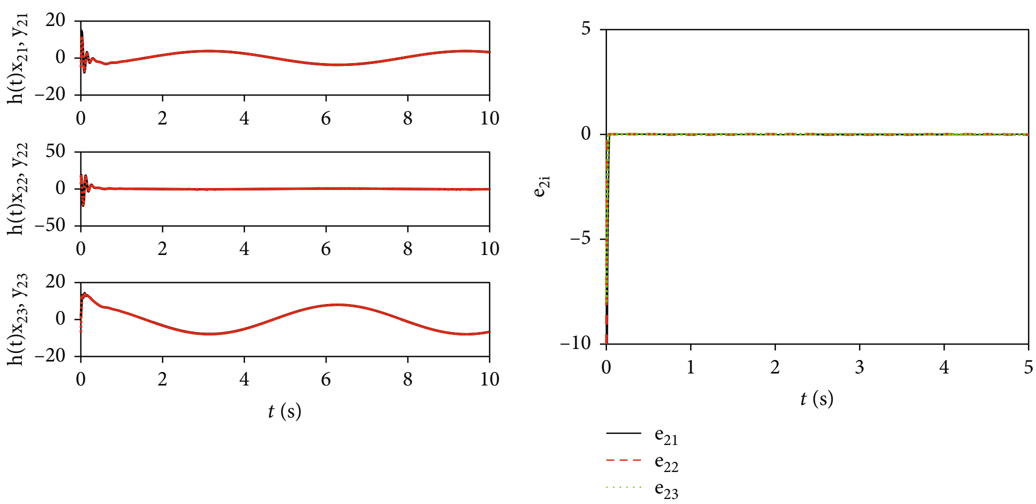

(a) Synchronization states $y_{2i}, h(t)x_{2i}$

(b) Synchronization errors e_{2i}

FIGURE 4: The time evolution of synchronization between y_{2i} and $h(t)x_{2i}$.

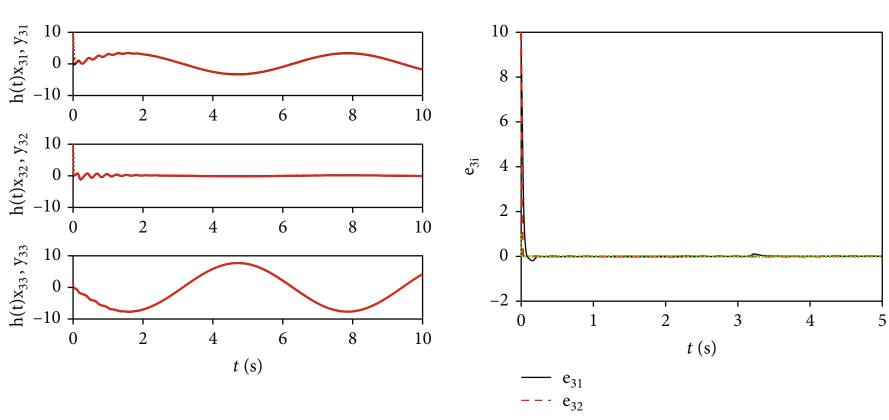

(a) Synchronization states $y_{3i}, h(t)x_{3i}$

(b) Synchronization errors e_{3i}

FIGURE 5: The time evolution of synchronization between y_{3i} and $h(t)x_{3i}$.

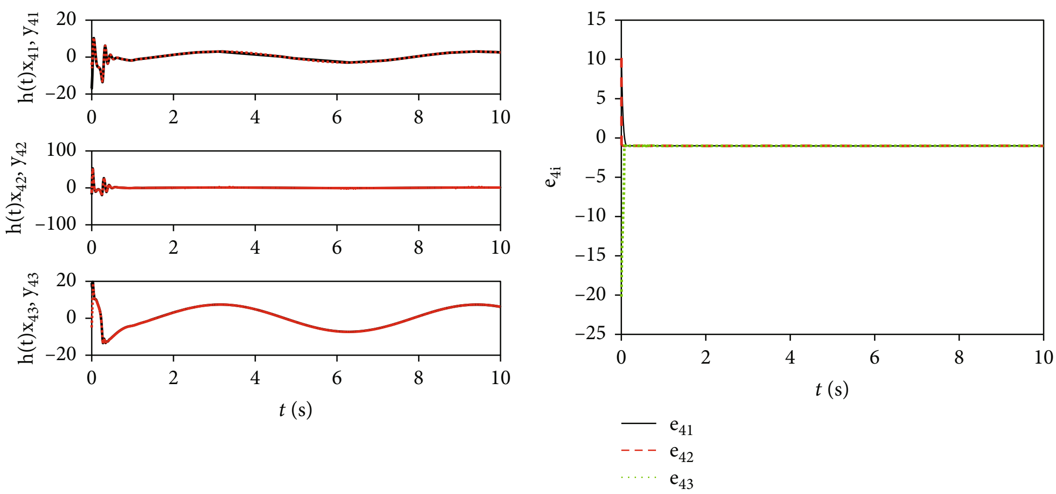

(a) Synchronization states $y_{4i}, h(t)x_{4i}$ (b) Synchronization errors e_{4i}

FIGURE 6: The time evolution of synchronization between y_{4i} and $h(t)x_{4i}$.

The MATLAB simulation results are shown in Figures 3–6. It displays that the error signal between the drive system and the response system can stably approach to zero with the designed adaptive controller, that is, the function projection synchronization of the complex dynamic networks is realized.

$$\begin{bmatrix} \dot{x}_{i1}(t) \\ \dot{x}_{i2}(t) \\ \dot{x}_{i3}(t) \\ \dot{x}_{i4}(t) \end{bmatrix} = \begin{bmatrix} 0 \\ -x_{i1}(t)x_{i3}(t) - x_{i2}(t) \\ x_{i1}(t)x_{i2}(t) \\ -x_{i1}(t) \end{bmatrix} + \begin{bmatrix} -x_{i1}(t) + x_{i2}(t) & 0 & x_{i4}(t) & 0 \\ 0 & x_{i1}(t) & 0 & 0 \\ 0 & 0 & 0 & -x_{i3}(t) \\ -x_{i4}(t) & 0 & 0 & 0 \end{bmatrix} \times \begin{bmatrix} \theta_{i1} \\ \theta_{i2} \\ \theta_{i3} \\ \theta_{i4} \end{bmatrix} + \begin{bmatrix} d_{i1}^{v}(t) \\ d_{i2}^{v}(t) \\ d_{i3}^{v}(t) \\ d_{i4}^{v}(t) \end{bmatrix} + c_0(t) \sum_{j=1}^{8} a_{ij}^{0} \Gamma_0 x_j(t) + c_1(t) \sum_{j=1}^{8} a_{ij}^{1} \Gamma_1 x_j(t - \tau_1(t)) + c_2(t) \sum_{j=1}^{8} a_{ij}^{2} \Gamma_2 x_j(t - \tau_2(t)) + c_3(t) \sum_{j=1}^{8} a_{ij}^{3} \Gamma_3 x_j(t - \tau_3(t)). \; i = 1, 2, \cdots, 8. \tag{34}$$

Example 2. Considering a communication network with $N = 8, n = 4$, the drive system is composed of eight LS hyperchaotic systems with three different time-varying delay couplings.

The response system is composed of four hyperchaotic systems with three different time-varying delay couplings.

$$\begin{bmatrix} \dot{y}_{i1}(t) \\ \dot{y}_{i2}(t) \\ \dot{y}_{i3}(t) \\ \dot{y}_{i4}(t) \end{bmatrix} = \begin{bmatrix} 0 \\ -y_{i1}(t)y_{i3}(t) + y_{i4}(t) \\ y_{i1}(t)y_{i2}(t) \\ 0 \end{bmatrix} + \begin{bmatrix} y_{i2}(t) - y_{i1}(t) & 0 & 0 & 0 \\ 0 & y_{i1}(t) & 0 & 0 \\ 0 & 0 & -y_{i3}(t) & 0 \\ 0 & 0 & 0 & -y_{i1}(t) \end{bmatrix} \times \begin{bmatrix} \eta_{i1} \\ \eta_{i2} \\ \eta_{i3} \\ \eta_{i4} \end{bmatrix} + \begin{bmatrix} d_{i1}^{s}(t) \\ d_{i2}^{s}(t) \\ d_{i3}^{s}(t) \\ d_{i4}^{s}(t) \end{bmatrix} + \begin{bmatrix} \phi_{i1}(u_{i1}(t)) \\ \phi_{i2}(u_{i2}(t)) \\ \phi_{i3}(u_{i3}(t)) \\ \phi_{i4}(u_{i4}(t)) \end{bmatrix} + c_0(t) \sum_{j=1}^{8} a_{ij}^{0} \Gamma_0 y_j(t) + c_1(t) \sum_{j=1}^{8} a_{ij}^{1} \Gamma_1 y_j(t - \tau_1(t)) + c_2(t) \sum_{j=1}^{8} a_{ij}^{2} \Gamma_2 y_j(t - \tau_2(t)) + c_3(t) \sum_{j=1}^{8} a_{ij}^{3} \Gamma_3 y_j(t - \tau_3(t)) i = 1, 2, \cdots, 8. \tag{35}$$

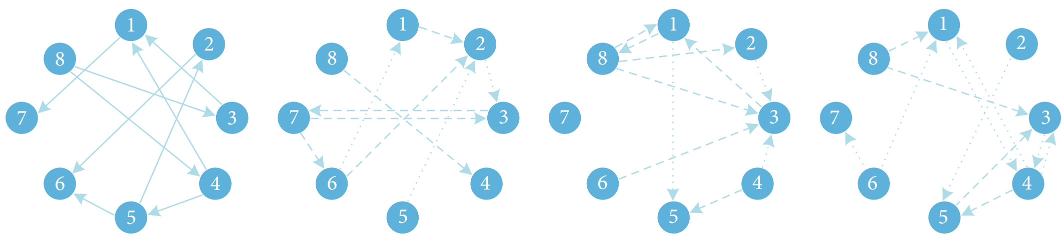

(a) $A0$ (b) $A1$ (c) $A2$ (d) $A3$

FIGURE 7: Topology of the multilink complex networks in Example 2 with eight nodes and four subnetworks.

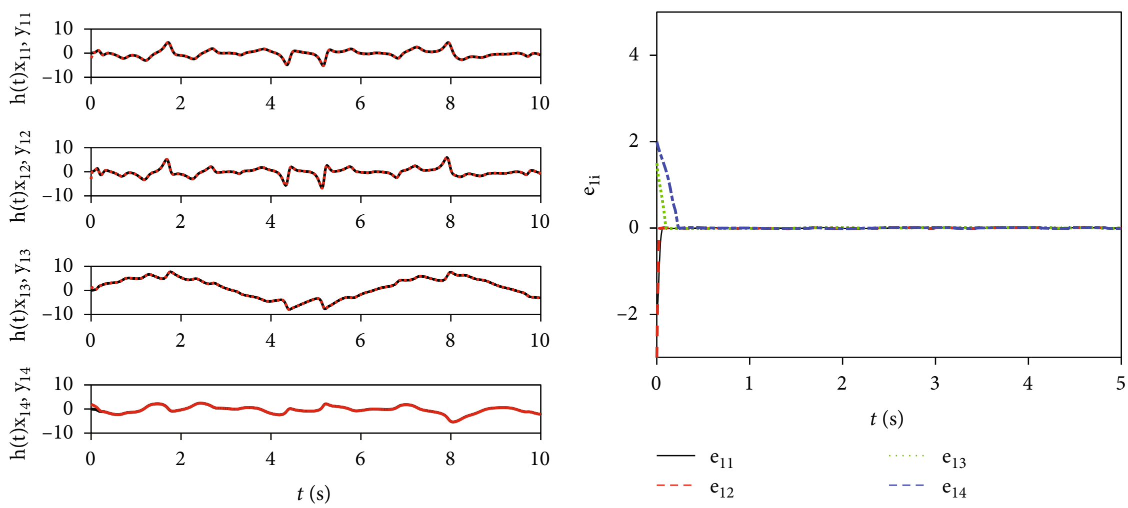

(a) Synchronization states $y_{1i}, h(t)x_{1i}$ (b) Synchronization errors e_{1i}

FIGURE 8: The time evolution of synchronization between y_{1i} and $h(t)x_{1i}$.

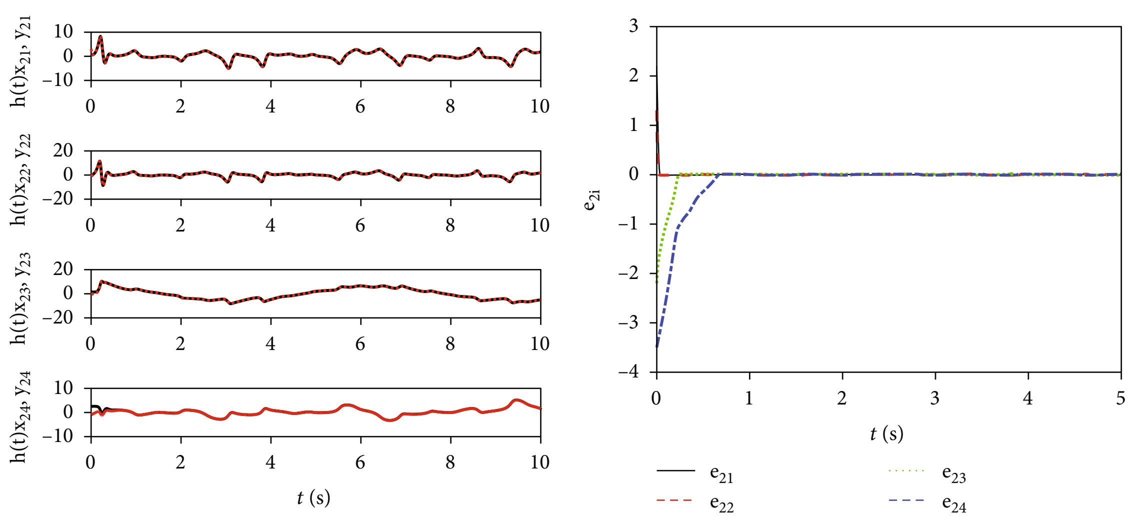

(a) Synchronization states $y_{2i}, h(t)x_{2i}$ (b) Synchronization errors e_{2i}

FIGURE 9: The time evolution of synchronization between y_{2i} and $h(t)x_{2i}$.

To simplify numerical simulation, set $c_0 = c_1 = c_2 = c_3 = 0.1$, $\tau_1(t) = t/3 + t$, $\tau_2(t) = e^t/3 + e^t$, $\tau_3(t) = e^t/6 + e^t$, $d_i(t) = 0.2 \sin t$, $\Gamma_0 = \Gamma_1 = \Gamma_2 = I^{4\times4}$, $h(t) = 2 \sin 2t$. The nonlinear input is $\phi_i(u_i(t)) = [\phi_{i1}(u_{i1}(t)), \phi_{i2}(u_{i2}(t)), \phi_{i3}(u_{i3}(t)), \phi_{i4}(u_{i4}(t))]^T = [(0.3 + 0.2 \cos(u_{i1}(t)))u_{i1}(t), (0.6 + 0.2 \sin(u_{i2}(t)))u_{i2}(t), (0.4 - 0.2 \cos(u_{i3}(t)))u_{i3}(t), (0.4 + 0.2 \sin(u_{i4}(t)))u_{i4}(t)]^T$. The topological structure matrices A_0, A_1, A_2, A_3 are as follows:

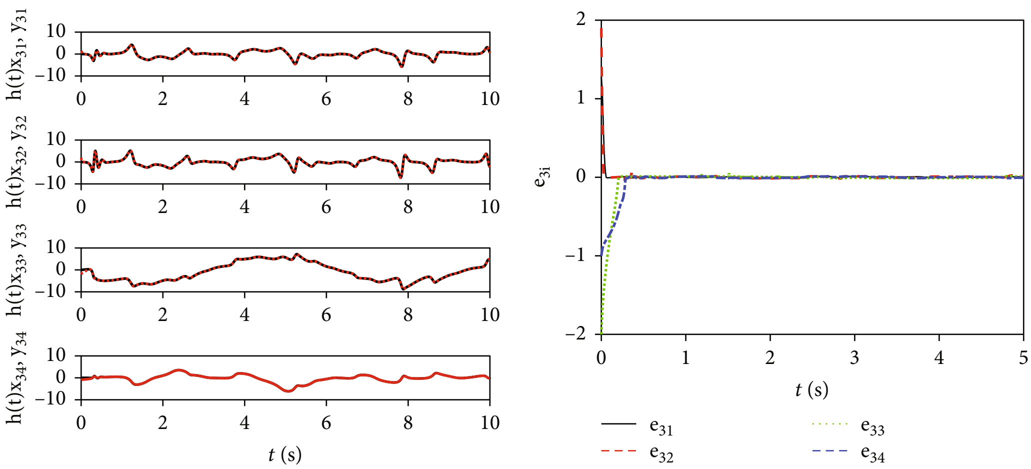

(a) Synchronization states $y_{3i}, h(t)x_{3i}$

(b) Synchronization errors e_{3i}

Figure 10: The time evolution of synchronization between y_{3i} and $h(t)x_{3i}$.

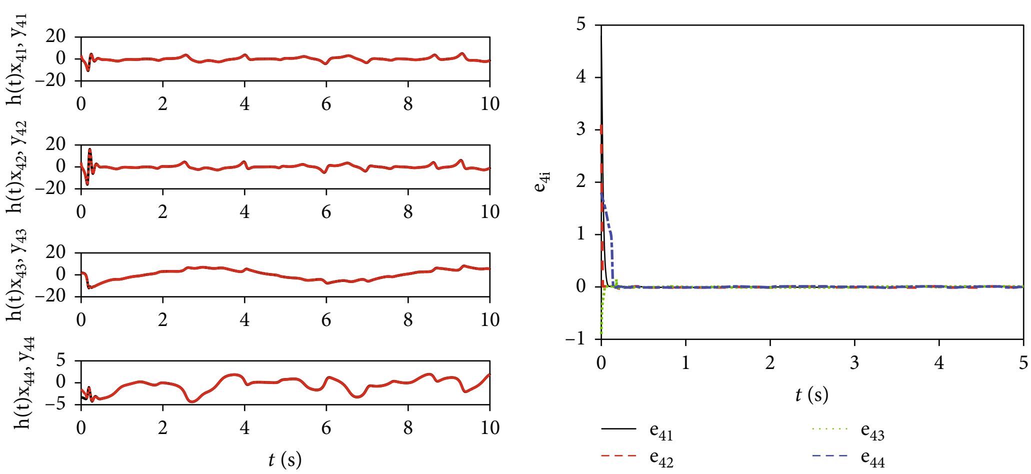

(a) Synchronization states $y_{4i}, h(t)x_{4i}$

(b) Synchronization errors e_{4i}

Figure 11: The time evolution of synchronization between y_{4i} and $h(t)x_{4i}$.

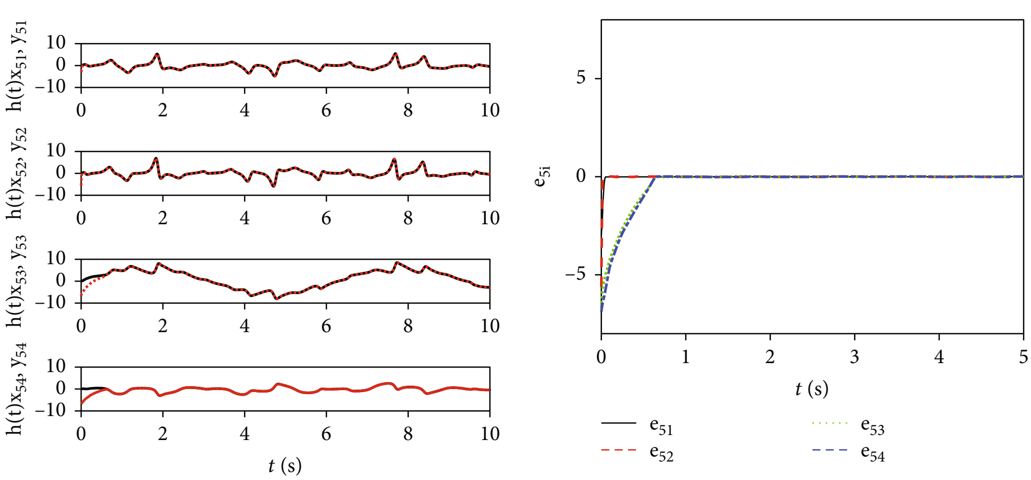

(a) Synchronization states $y_{5i}, h(t)x_{5i}$

(b) Synchronization errors e_{5i}

Figure 12: The time evolution of synchronization between y_{5i} and $h(t)x_{5i}$.

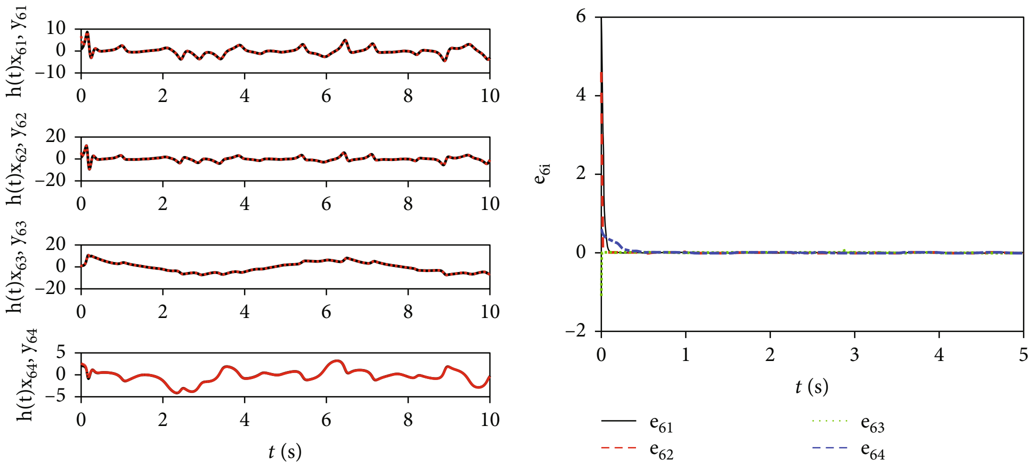

(a) Synchronization states $y_{6i}, h(t)x_{6i}$ (b) Synchronization errors e_{6i}

Figure 13: The time evolution of synchronization between y_{6i} and $h(t)x_{6i}$.

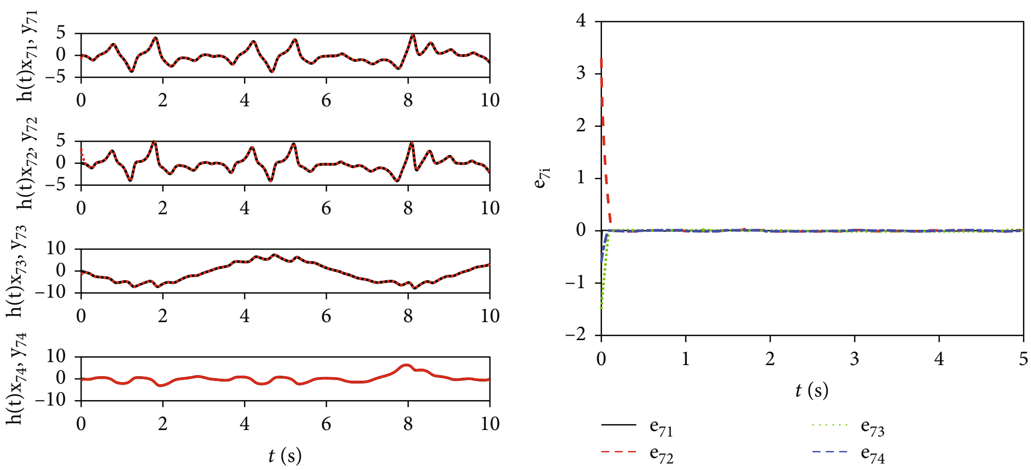

(a) Synchronization states $y_{7i}, h(t)x_{7i}$ (b) Synchronization errors e_{7i}

Figure 14: The time evolution of synchronization between y_{7i} and $h(t)x_{7i}$.

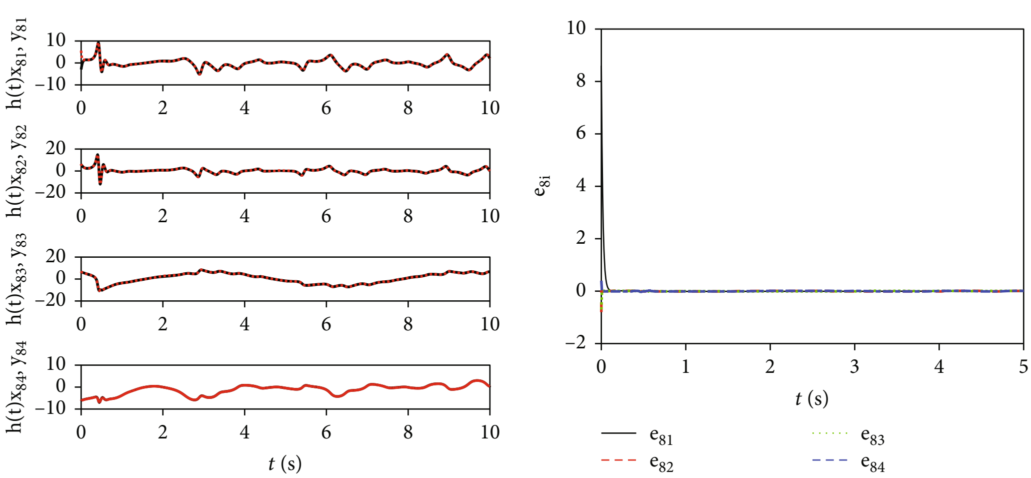

(a) Synchronization states $y_{8i}, h(t)x_{8i}$ (b) Synchronization errors e_{8i}

Figure 15: The time evolution of synchronization between y_{8i} and $h(t)x_{8i}$.

$$A_0 = \begin{pmatrix} -1 & 0 & 0 & 0 & 0 & 0 & 1 & 0 \\ 0 & -1 & 0 & 0 & 0 & 1 & 0 & 0 \\ 1 & 0 & -1 & 0 & 0 & 0 & 0 & 0 \\ 1 & 0 & 0 & -2 & 1 & 0 & 0 & 0 \\ 0 & 1 & 0 & 0 & -2 & 1 & 0 & 0 \\ 0 & 0 & 0 & 0 & 0 & 0 & 0 & 0 \\ 0 & 0 & 0 & 0 & 0 & 0 & 0 & 0 \\ 0 & 0 & 1 & 1 & 0 & 0 & 0 & -2 \end{pmatrix},$$
$$A_1 = \begin{pmatrix} -1 & 1 & 0 & 0 & 0 & 0 & 0 & 0 \\ 0 & -1 & 1 & 0 & 0 & 0 & 0 & 0 \\ 0 & 0 & -1 & 0 & 0 & 0 & 1 & 0 \\ 0 & 0 & 0 & 0 & 0 & 0 & 0 & 0 \\ 0 & 1 & 0 & 0 & -1 & 0 & 0 & 0 \\ 1 & 1 & 0 & 0 & 0 & -2 & 0 & 0 \\ 0 & 0 & 1 & 0 & 0 & 1 & -2 & 0 \\ 0 & 0 & 0 & 1 & 0 & 0 & 0 & -1 \end{pmatrix},$$
$$A_2 = \begin{pmatrix} -2 & 0 & 0 & 0 & 1 & 0 & 0 & 1 \\ 0 & -1 & 1 & 0 & 0 & 0 & 0 & 0 \\ 1 & 0 & -1 & 0 & 0 & 0 & 0 & 0 \\ 0 & 0 & 1 & -2 & 1 & 0 & 0 & 0 \\ 0 & 0 & 0 & 0 & 0 & 0 & 0 & 0 \\ 0 & 0 & 1 & 0 & 0 & -1 & 0 & 0 \\ 0 & 0 & 0 & 0 & 0 & 0 & 0 & 0 \\ 1 & 1 & 1 & 0 & 0 & 0 & 0 & -3 \end{pmatrix},$$
$$A_3 = \begin{pmatrix} -1 & 0 & 0 & 1 & 0 & 0 & 0 & 0 \\ 0 & -1 & 0 & 0 & 1 & 0 & 0 & 0 \\ 0 & 0 & -1 & 1 & 0 & 0 & 0 & 0 \\ 1 & 0 & 1 & -3 & 1 & 0 & 0 & 0 \\ 0 & 0 & 1 & 0 & -1 & 0 & 0 & 0 \\ 1 & 0 & 0 & 0 & 0 & -2 & 1 & 0 \\ 0 & 0 & 0 & 0 & 0 & 0 & 0 & 0 \\ 1 & 0 & 1 & 0 & 0 & 0 & 0 & -2 \end{pmatrix}. \tag{36}$$

And the topology of the driver network and response network is shown in Figure 7.

The MATLAB simulation results are shown in Figures 8–15. The function projection synchronization can still be achieved when the number of nodes and the system dimension of the complex network are increased, which further verifies the correctness of the theoretical analysis.

5. Conclusion

In this paper, the function projective synchronization of complex dynamic networks with unknown sector nonlinear input, multiple time-varying delay couplings, model uncertainty, and external interferences is studied. Based on Lyapunov stability theory, adaptive control theory, and inequality theory, the robust adaptive controller is formulated to make the drive and response systems synchronize by the function scaling factor. The controller designed in this paper can effectively overcome the effects of unknown sector input and multiple time-varying delays, so it is more general and easier to implement. Our future research work will focus on how to realize the complex network synchronization with other forms of input constraints and how to apply the research results of this paper to the fields of information security.

Data Availability

No data were used to support this study.

Conflicts of Interest

The authors declare that they have no conflicts of interest.

Acknowledgments

The work was supported in part by the National Natural Science Foundation of China (Grant no. 61775198) and Henan Province Science and Technology research project (Grant nos. 222102210266 and 222102210059).

References

[1] R. R. Cheng, M. S. Peng, J. C. Yu, and H. F. Li, "Synchronization for discrete-time complex networks with probabilistic time delays," *Physica A: Statistical Mechanics and its Applications*, vol. 525, no. C, article S0378437119303760, pp. 1088–1101, 2019.

[2] P. Li, B. Y. Li, J. Mou, and C. F. Luo, "Chaos synchronization of complex network based on signal superposition of single variable," *International Journal of Wireless Information Networks*, vol. 25, no. 3, article 386, pp. 258–268, 2018.

[3] W. L. Lu and T. P. Chen, "QUAD-condition, synchronization, consensus of multiagents, and anti-synchronization of complex networks," *IEEE Transactions on Cybernetics*, vol. 51, no. 6, pp. 3384–3388, 2021.

[4] D. Ding, Z. Tang, Y. Wang, and Z. C. Ji, "Synchronization of nonlinearly coupled complex networks: distributed impulsive method," *Chaos, Solitons and Fractals*, vol. 133, article S0960077920300199, p. 109620, 2020.

[5] Y. B. Wu, H. Z. Li, and W. X. Li, "Intermittent control strategy for synchronization analysis of time-varying complex

dynamical networks," *IEEE Transactions on Systems, Man, and Cybernetics: Systems*, vol. 51, no. 5, pp. 3251–3262, 2021.

[6] X. X. Lv, J. D. Cao, X. D. Li, M. Abdel-Aty, and U. A. Al-Juboori, "Synchronization analysis for complex dynamical networks with coupling delay via event-triggered delayed impulsive control," *IEEE transactions on cybernetics*, vol. 51, no. 11, pp. 5269–5278, 2021.

[7] T. T. Hu, Z. He, X. J. Zhang, S. Zhong, K. Shi, and Y. Zhang, "Adaptive fuzzy control for quasi-synchronization of uncertain complex dynamical networks with time-varying topology via event-triggered communication strategy," *Information Sciences*, vol. 582, article S0020025521010446, pp. 704–724, 2022.

[8] L. H. Zhao and J. L. Wang, "LagH∞synchronization and lag synchronization for multiple derivative coupled complex networks," *Neurocomputing*, vol. 384, article S0925231219317047, pp. 46–56, 2020.

[9] L. Wang, H. P. Dai, and Y. X. Sun, "Synchronization criteria for a generalized complex delayed dynamical network model," *Physica A: Statistical Mechanics and its Applications*, vol. 383, no. 2, article S0378437107002944, pp. 703–713, 2007.

[10] M. Zhang and M. Han, "Finite-time combination synchronization of uncertain complex networks based on sliding mode control method," *Control and Decision*, vol. 32, no. 8, pp. 1533–1536, 2017.

[11] Z. R. Heydari and P. Karimaghaee, "Projective synchronization of different uncertain fractional-order multiple chaotic systems with input nonlinearity via adaptive sliding mode control," *Advances in Difference Equations*, vol. 2019, 23 pages, 2019.

[12] X. J. Wu and H. T. Lu, "Generalized function projective (lag, anticipated and complete) synchronization between two different complex networks with nonidentical nodes," *Communications in Nonlinear Science and Numerical Simulation*, vol. 17, no. 7, article S1007570411006058, pp. 3005–3021, 2012.

[13] X. L. Qiu, W. S. Lin, and Y. M. Zheng, "Function projective synchronization of complex networks with distributed delays via hybrid feedback control," *IEEE Access*, vol. 8, pp. 99110–99114, 2020.

[14] H. Y. Du, P. Shi, and N. Lü, "Function projective synchronization in complex dynamical networks with time delay via hybrid feedback control," *Nonlinear Analysis: Real World Applications*, vol. 14, no. 2, article S1468121812002064, pp. 1182–1190, 2013.

[15] Y. G. Jin and S. M. Zhong, "Function projective synchronization in complex networks with switching topology and stochastic effects," *Applied Mathematics and Computation*, vol. 259, article S0096300315002805, pp. 730–740, 2015.

[16] W. P. Wang, H. P. Peng, L. X. Li, J. H. Xiao, and Y. X. Yang, "Finite-time function projective synchronization in complex multi-links networks with time-varying delay," *Neural Processing Letters*, vol. 41, no. 1, article 9335, pp. 71–88, 2015.

[17] L. Z. Gan, S. Li, N. Duan, and X. Y. Kong, "Adaptive output synchronization of general complex dynamical network with time-varying delays," *Mathematics*, vol. 8, no. 3, p. 311, 2020.

[18] P. He, X. L. Wang, and Y. M. Li, "Guaranteed cost synchronization of complex networks with uncertainties and time-varying delays," *Complexity*, vol. 21, 395 pages, 2016.

[19] M. S. Ali, J. Yogambigai, and J. D. Cao, "Synchronization of master-slave Markovian switching complex dynamical networks with time-varying delays in nonlinear function via sliding mode control," *Acta Mathematica Scientia*, vol. 37, no. 2, article S0252960217300085, pp. 368–384, 2017.

[20] H. G. Fan, K. B. Shi, and Y. Zhao, "Pinning impulsive cluster synchronization of uncertain complex dynamical networks with multiple time-varying delays and impulsive effects," *Physica A: Statistical Mechanics and its Applications*, vol. 587, article S0378437121008074, p. 126534, 2022.

[21] J. Fang, N. Liu, and J. W. Sun, "Adaptive modified function projective synchronization of uncertain complex dynamical networks with multiple time-delay couplings and disturbances," *Mathematical Problems in Engineering*, vol. 2018, 11 pages, 2018.

[22] C. Zhang, X. Y. Wang, C. P. Wang, and W. J. Zhou, "Synchronization of uncertain complex networks with time-varying node delay and multiple time-varying coupling delays," *Asian Journal of Control*, vol. 20, no. 1, pp. 186–195, 2018.

[23] C. Zhang, X. Y. Wang, C. P. Wang, and Z. Liu, "Synchronization in nonlinear complex networks with multiple time-varying delays via adaptive aperiodically intermittent control," *International Journal of Adaptive Control and Signal Processing*, vol. 33, no. 1, pp. 39–51, 2019.

[24] X. Wang, K. She, S. M. Zhong, and H. L. Yang, "Lag synchronization analysis of general complex networks with multiple time-varying delays via pinning control strategy," *Neural Computing & Applications*, vol. 31, no. 1, article 2978, pp. 43–53, 2019.

[25] Y. P. Zhao, P. He, H. S. Nik, and J. C. Ren, "Robust adaptive synchronization of uncertain complex networks with multiple time-varying coupled delays," *Complexity*, vol. 20, 73 pages, 2015.

[26] Y. M. Lu, P. He, S. H. Ma, G. Z. Li, and S. Mobayben, "Robust adaptive synchronization of general dynamical networks with multiple delays and uncertainties," *Pramana-Journal of Physics*, vol. 86, no. 6, article 1182, pp. 1223–1241, 2016.

[27] Z. H. Guan, Z. W. Liu, G. Feng, and Y. W. Wang, "Synchronization of complex dynamical networks with time-varying delays via impulsive distributed control," *IEEE Transactions on Circuits and Systems I: Regular Papers*, vol. 57, no. 8, pp. 2182–2195, 2010.

[28] C. H. Lin, G. H. Hu, and J. J. Yan, "Chaos suppression in uncertain generalized Lorenz-Stenflo systems via a single rippling controller with input nonlinearity," *Mathematics*, vol. 8, no. 3, p. 327, 2020.

[29] A. Shafiq, A. B. Colak, S. A. Lone, T. N. Sindhu, and T. Muhammad, "Reliability modeling and analysis of mixture of exponential distributions using artificial neural network," in *Mathematical Methods in the Applied Sciences*, Wiley Online Library, 2022.

[30] S. L. Zhu, D. Y. Duan, L. Chu, M. X. Wang, Y. Q. Han, and P. C. Xiong, "Adaptive multi-dimensional Taylor network tracking control for a class of switched nonlinear systems with input nonlinearity," *Transactions of the Institute of Measurement and Control*, vol. 42, no. 13, pp. 2482–2491, 2020.

[31] M. C. Pai, "Sliding mode control for discrete-time chaotic systems with input nonlinearity," *Journal of Dynamic Systems, Measurement, and Control*, vol. 142, no. 10, p. 101003, 2020.

[32] C. G. Liu, X. P. Liu, H. Q. Wang, S. Y. Lu, and Y. C. Zhou, "Adaptive control and application for nonlinear systems with input nonlinearities and unknown virtual control coefficients," *IEEE Transactions on Cybernetics*, vol. 3, pp. 1–14, 2021.

[33] T. N. Sindhu and A. Atangana, "Reliability analysis incorporating exponentiated inverse Weibull distribution and inverse power law," *Quality and Reliability Engineering International*, vol. 37, no. 6, pp. 2399–2422, 2021.

[34] M. Shirkavand and M. R. Soltanpour, "A novel robust fixed time synchronization of complex network subject to input nonlinearity in the presence of uncertainties and external disturbances," *Journal of Central South University*, vol. 27, no. 2, article 4306, pp. 418–431, 2020.

[35] A. Boulkroune and M. Msaad, "A fuzzy adaptive variable-structure control scheme for uncertain chaotic MIMO systems with sector nonlinearities and dead-zones," *Expert Systems with Applications*, vol. 38, no. 12, article S0957417411007895, pp. 14744–14750, 2011.

[36] J. Fang, Y. Jiang, and C. S. Jiang, "Modified projective synchronization of chaotic systems with unknown sector nonlinear input," *Journal of Basic Science and Engineering*, vol. 21, no. 2, pp. 379–390, 2013.

[37] A. Boubellouta, F. Zouari, and A. Boulkroune, "Intelligent fuzzy controller for chaos synchronization of uncertain fractional-order chaotic systems with input nonlinearities," *International Journal of General Systems*, vol. 48, no. 3, pp. 211–234, 2019.

[38] X. Y. Wang and M. Liu, "Sliding mode control for the synchronization of master-slave chaotic systems with sector nonlinear input," *Acta Photonica Sinica*, vol. 54, no. 6, article w20050624, pp. 2584–2589, 2005.

[39] C. H. Yang, K. C. Wang, L. Wu, and R. Wen, "State synchronization for a class of N-dimensional nonlinear systems with sector input nonlinearity via adaptive two-stage sliding mode control," *Mathematical Problems in Engineering*, vol. 2020, Article ID 5391984, 2020.

[40] J. Fang, D. Y. Xu, J. W. Sun, and W. Wang, "Adaptive modified function projective synchronization for uncertain complex dynamic networks with multiple time-varying delay couplings under input nonlinearity," *IEEE Access*, vol. 8, pp. 127393–127403, 2020.